The Effect of Flat Plate Theory Assumption in Post-Stall Lift and Drag Coefficients Extrapolation with Viterna Method

Faisal Mahmuddin^{a,*}

^{a)}Marine Engineering Department, Engineering Faculty, Hasanuddin University, Makassar Indonesia

*Corresponding author: f.mahmuddin@gmail.com

Paper History

Received: 25-June-2016

Received in revised form: 28-June-2016

Accepted: 30-June-2016

ABSTRACT

In employing blade element momentum (BEM) method to compute the performance of a turbine propeller, the lift and drag coefficients of propeller element/airfoil are needed. The coefficients are usually obtained from model experiment. Unfortunately, the model experiment can only be conducted for small angle of attack until stall mode. Beyond stall mode, Viterna extrapolation method is commonly used. The method is used to predict the lift and drag coefficients from stall angle to 90°. Beyond that range, besides Viterna method, original flat plate theory assumption can also be adopted. The present study compares the lift and drag coefficients extrapolation using Viterna method and flat plat theory. NACA2415 airfoil shape is used for computation. The computation formulas and procedures are presented and important parameter effect to the coefficients are shown and explained.

KEY WORDS: Blade Element Momentum, Experimental Data Extrapolation, Flat Plate Theory, Lift and Drag Coefficients, NACA2415, Viterna Method.

NOMENCLATURE

AR aspect ratio AoA angle of Attack C_D drag coefficient C_L lift coefficient

 α angle of attack

1.0 INTRODUCTION

One of popular methods to predict the power produced by a wind turbine is blade element momentum (BEM) method. The main advantages of the method are simple formulation, fast computation, and good accuracy results especially for steady state condition. Examples of BEM method application can be found in references (Ceyhan, 2008; Døssing, Madsen, & Bak, 2011; Godreau, Caldeira, & Campos, n.d.; Liu & Janajreh, 2012).

In this method, the propeller blade is divided into several elements/airfoil. Each element is assumed to act independently and has no interaction between them. The forces and moments are computed on each element/airfoil. The total forces and moments are obtained by integrating the forces and moments on each element/airfoil.

Therefore, in order to use the BEM method, each element/airfoil performance in terms of lift and drag coefficients is necessary. The performance is usually obtained by conducting a model experiment. However, the model experiments can only be conducted for small angle of attack (*AoA*) until stall mode. For post stall mode performance, it necessary to extrapolate the data obtained from the model experiment in order to obtain the full 360° data

For obtaining the full polar data, several extrapolation methods can be used such as Bean and Jakubowski correlation, Kirke Correlation, Montgomerie model, Viterna model, etc. (Bianchini et al., 2016). Of the methods, Viterna model is the most common one to be used because it can be implemented more straightforwardly with reliable results.

The Viterna method is used specifically to be implemented to predict the lift and drag coefficients from stall mode to 90° of AoA. For AoA higher than 90° , formulation based on the original flat plate theory can also be implemented.

The present study compares the data extrapolation results computed using Viterna method and original flat plate theory. The computation formulas and procedures of both

implementation methods are presented and important parameter effect to coefficients are shown and explained. For demonstrating the calculation procedures, an airfoil based on NACA2415 shape is used.

2.0 SOLUTION METHOD

In the present study, the Viterna method is used to extrapolate the lift and drag coefficients beyond the stall angle until 90o. Beyond that range, original flat plate theory assumption can also be adopted.

2.1 Viterna Method

The Viterna method, also known as Viterna-Corrigan method, is a data extrapolation method for AoA (a) greater than stall angle (α_{stall}) but less than or equal to 90°. The method was formulated by utilizing flat plate theory (Matthew, 2009). It requires an initial angle with its associated drag and lift coefficients which should satisfy flat plate theory.

The Viterna method is formulated to extrapolate the lift and drag coefficients using the following equation (L. A. Viterna & Janetzke, 1982; L. Viterna & Corrigan, 1982):

$$C_L = A_1 \sin 2\alpha + A_2 \frac{\cos^2 \alpha}{\sin \alpha} \tag{1}$$

$$C_D = B_1 \sin^2 \alpha + B_2 \cos \alpha \tag{2}$$

where

$$A_{1} = \frac{C_{D_{max}}}{2} \tag{3}$$

$$B_1 = C_{D_{max}}(4) A_2 = \left(C_{L_{stall}} - C_{D_{max}} \sin \alpha_{stall} \cos \alpha_{stal}\right)$$

$$B_2 = \frac{C_{D_{stall}} - C_{D_{max}} \sin^2 \alpha_{stall}}{\cos \alpha_{stall}}$$
(6)

 C_{Dmax} is found using aspect ratio (AR) as follows

$$C_D = \Box 1.11 + 0.018AR$$
 (7)

The AR in Eq. (7) can be obtained from BEM method application where finite blade length will affects the flat plate assumption. The chosen value of AR will not affect the results significantly. AR equals to 9-10 can be used for most computations.

For data extrapolation from $\alpha > 90^{\circ}$ to $\alpha < \alpha_{min}$, the calculated values are reflected. The Viterna method does not consider pressure or skin friction distributions; however, by making a few simple assumptions and correction, it is possible to obtain a reasonable estimate from the Viterna method. While the method is not an accurate representation of the true physics, it provides a reasonable estimate and accuracy in early design process.

2.2 Flat Plate Theory

It is known from flat plate theory that for deep stall or high angle of attack region (greater than 20°), the upper surface of the airfoil receives no direct impact from the flow due to flow separation. The condition is consistent with what so-called Newtonian Flow condition. Consequently, the thickness of the airfoil can be neglected. In this deep stall region, lift and drag coefficients are largely independent of airfoil geometry but mainly depends on the blade geometry and aspect ratio (J. L. Tangler, 2004).

Moreover, the flow of lower surface is completely laminar, and its contribution to the overall drag force is very small. Therefore, when the foil in high angle of attack position, the foil will behave like a thin of flat plate.

When assuming that the airfoil behave like a flat plate for deep stall angle, the flow separation effect will exist. Therefore, in order to resolve the flat plate flow behaviour, the stagnation point on the rear side of the airfoil is moved by assuming potential flow theory like behaviour. Based on the principle, the curve of lift and drag coefficients can be described using the following equations (Duquette, 2007; J. Tangler & Kocurek, 2005; Timmer, 2010).

$$C_L = 2\sin\alpha\cos\alpha \tag{8}$$

$$C_D = 2\sin^2\alpha \tag{9}$$

It can be implied from Eq. (8) and (9) that lift and drag coefficients at $\alpha = 0$ will be zero. This is idealization of the curve and not realistic. Even though not realistic, the theory assumption was found to be a good first-order approximation of lift and drag coefficients (Hoburg & Tedrake, 2009).

2.2 4 (four) Digits NACA Airfoil

 $B_1 = C_{D_{max}} \text{ (4) } A_2 = \left(C_{L_{stall}} - C_{D_{max}} \sin \alpha_{stall} \cos \alpha_{stall}^{-1} \cos \alpha_{stall}^{$ and systematic shapes. Based on the shapes, NACA established the shape nomenclature which is now a well-known standard (Tobergte & Curtis, 2013).

Original NACA airfoil series consists the 4-digit, 5-digit, and modified 4-/5-digit which can be drawn using analytical equations that involve the camber (curvature) of the mean-line (geometric centreline) of the airfoil section as well as the section's thickness distribution along the airfoil length. Later series has included the 6-digit series which are more complicated shapes constructed using theoretical rather than geometrical methods.

The 4-digit series are first family of NACA series airfoil. The first digit specifies the maximum camber (m) in percentage of the chord (c), the second indicates the position of the maximum camber (p) in tenths of chord, and the last two digits provide the maximum thickness (t) of the airfoil in percentage of chord. For example, the NACA2415 airfoil, which is the one used in the present study, means the airfoil has a maximum thickness of 15% (0.15c) with a camber of 2% (0.02c) located 40% (0.4c) back from the airfoil leading edge. By knowing the values of m, p, and t, the coordinates and shape of an airfoil can be computed and drawn.

3.0 AIRFOIL DATA

The computed airfoil shape in the present study is NACA2415. Using the definition of 4 (four) digits NACA airfoil described in the previous section, the shape of the airfoil is drawn and shown in the following figure

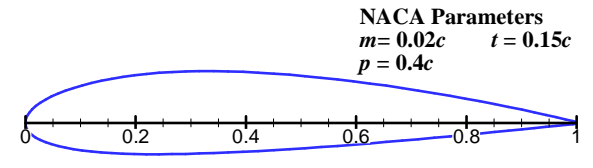
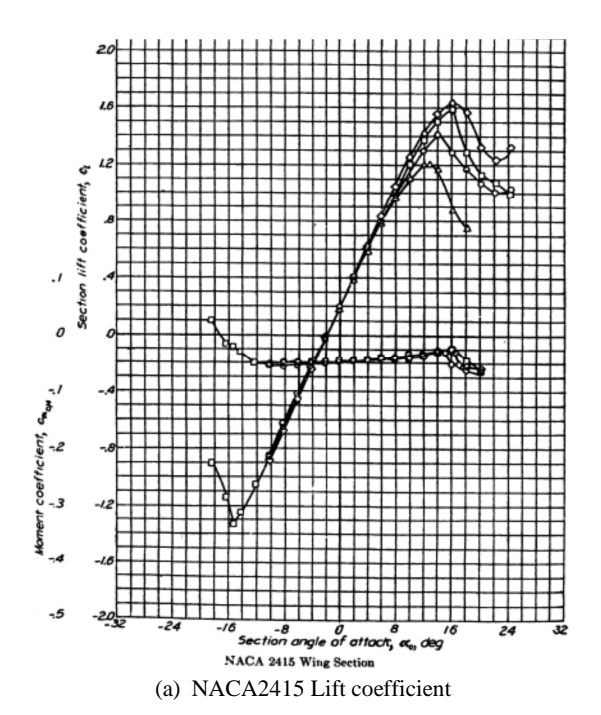


Figure 1: NACA2415 airfoil shape

The lift and drag coefficients of the airfoil will be the input data for the program code. The coefficients of the airfoil will be mostly taken from experiment data which can be found in reference (Abbott & Doenhoff, 1949). The experimental results are shown in the following graphs.



3.020
3.020
3.020
3.020
3.020
3.020
3.020
3.020
3.020
3.020
3.020
3.020
3.020
3.020
3.020
3.020
3.020
3.020
3.020
3.030
3.030
3.030
3.030
3.030
3.030
3.030
3.030
3.030
3.030
3.030
3.030
3.030
3.030
3.030
3.030
3.030
3.030
3.030
3.030
3.030
3.030
3.030
3.030
3.030
3.030
3.030
3.030
3.030
3.030
3.030
3.030
3.030
3.030
3.030
3.030
3.030
3.030
3.030
3.030
3.030
3.030
3.030
3.030
3.030
3.030
3.030
3.030
3.030
3.030
3.030
3.030
3.030
3.030
3.030
3.030
3.030
3.030
3.030
3.030
3.030
3.030
3.030
3.030
3.030
3.030
3.030
3.030
3.030
3.030
3.030
3.030
3.030
3.030
3.030
3.030
3.030
3.030
3.030
3.030
3.030
3.030
3.030
3.030
3.030
3.030
3.030
3.030
3.030
3.030
3.030
3.030
3.030
3.030
3.030
3.030
3.030
3.030
3.030
3.030
3.030
3.030
3.030
3.030
3.030
3.030
3.030
3.030
3.030
3.030
3.030
3.030
3.030
3.030
3.030
3.030
3.030
3.030
3.030
3.030
3.030
3.030
3.030
3.030
3.030
3.030
3.030
3.030
3.030
3.030
3.030
3.030
3.030
3.030
3.030
3.030
3.030
3.030
3.030
3.030
3.030
3.030
3.030
3.030
3.030
3.030
3.030
3.030
3.030
3.030
3.030
3.030
3.030
3.030
3.030
3.030
3.030
3.030
3.030
3.030
3.030
3.030
3.030
3.030
3.030
3.030
3.030
3.030
3.030
3.030
3.030
3.030
3.030
3.030
3.030
3.030
3.030
3.030
3.030
3.030
3.030
3.030
3.030
3.030
3.030
3.030
3.030
3.030
3.030
3.030
3.030
3.030
3.030
3.030
3.030
3.030
3.030
3.030
3.030
3.030
3.030
3.030
3.030
3.030
3.030
3.030
3.030
3.030
3.030
3.030
3.030
3.030
3.030
3.030
3.030
3.030
3.030
3.030
3.030
3.030
3.030
3.030
3.030
3.030
3.030
3.030
3.030
3.030
3.030
3.030
3.030
3.030
3.030
3.030
3.030
3.030
3.030
3.030
3.030
3.030
3.030
3.030
3.030
3.030
3.030
3.030
3.030
3.030
3.030
3.030
3.030
3.030
3.030
3.030
3.030
3.030
3.030
3.030
3.030
3.030
3.030
3.030
3.030
3.030
3.030
3.030
3.030
3.030
3.030
3.030
3.030
3.030
3.030
3.030
3.030
3.030
3.030
3.030
3.030
3.030
3.030
3.030
3.030
3.030
3.030
3.030
3.030
3.030
3.030
3.030
3.030
3.030
3.030
3.030
3.030
3.030
3.030
3.030
3.030
3.030
3.030
3.030
3.030
3.030
3.030
3.030
3.030
3.030
3.030
3.030
3.030
3.030
3.030
3.030
3.030
3.030
3.030
3.030
3.030
3.030
3.030
3.030

Figure 2: NACA2415 Lift and Drag Coefficients (Abbott & Doenhoff, 1949)

However, it can be seen from Fig. 2 that after AoA of 15.95° , the C_D cannot be determined from experimental graph. Therefore, in order to resolve the issue, a polynomial fit will be used to predict the value of C_D for this range. The same procedure has also been demonstrated in reference (McCosker, 2012).

For the present case, 3^{rd} order polynomial is used to predict the C_D for unknown C_D range. By using the available data, the equation of the polynomial can be determined and shown as

$$8 \cdot 10^{-7} x^3 + 4 \cdot 10^{-5} x^2 + 6 \cdot 10^{-5} x + 0.0063$$
 (10)

The summary of C_L and C_D data obtained from experiment curve and predicted by Eq. (10) are shown in the following table

Table 1: NACA2415 Lift and drag coefficients

Table 1. NACA2413 Lift and drag coefficients			
AoA (degree)	C_L	C_D	
-10.34	-0.86	0.00905	
-8.27	-0.64	0.00786	
-6.2	-0.42	0.00718	
-4.34	-0.24	0.00676	
-2.27	-0.02	0.00647	
-0.2	0.2	0.00648	

24.27

1.87	0.41	0.00651
3.94	0.61	0.00699
5.59	0.84	0.00799
7.66	1.06	0.00935
9.73	1.27	0.01116
11.8	1.43	0.01368
13.66	1.57	0.01613
15.95	1.65	0.019722
18.03	1.59	0.023992
20.12	1.34	0.029008

In order to observe more clearly the input data, the data shown in the above table is shown in graph below.

1.34

0.034766

0.041298

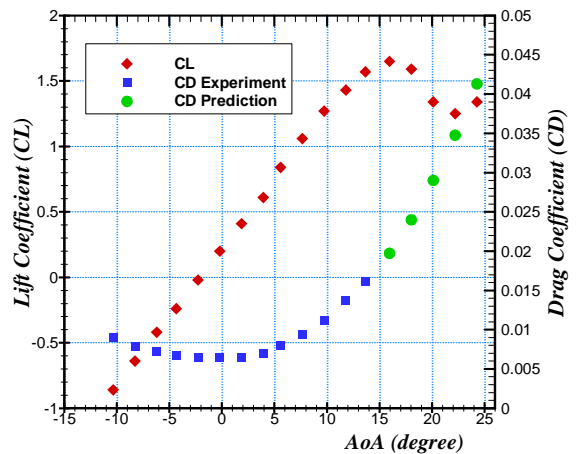


Figure 3: Experimental and predicted C_D and C_L

As shown in the above graph, stall angle is around 15° of AoA. Unfortunately, as described before, the C_D data are not available for post-stall angle. Therefore, they are predicted using polynomial equation shown in Eq. (10). The predicted C_D data are shown as green circle symbol in Fig. 3.

4.0 RESULTS AND DISCUSSION

Based on the airfoil C_D and C_L coefficients shown in Table. 1, computations are performed using the methods described in the preceding section. The first computation is performed to analyse the effect of Coefficient lift adjustment (C_{Ladj}) to lift coefficient. The C_{Ladj} is an important parameter needs to be determined when using the Viterna method to predict the lift and drag coefficients beyond the range from stall angle to 90° . C_{Ladj} will determine the maximum value of computed C_L .

3 (three) values of C_{Ladj} are used which are $C_{Ladj} = 0.7, 0.9$, and 1.2. The computation results are shown in the following figure

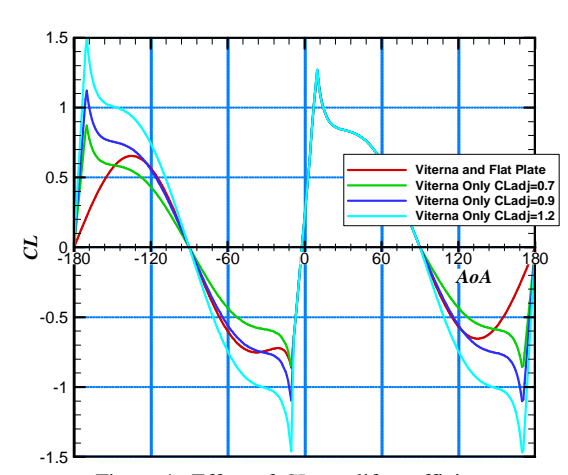


Figure 4: Effect of CL_{adj} to lift coefficient

From figure, it can be seen that $C_{Ladj} = 0.9$ has the best fit to the line compared to other values of C_{Ladj} . Therefore, the next computation will use $C_{Ladj} = 0.9$.

The next computation is performed to analyse the extrapolation of C_L using Viterna method only and flat plate theory assumption. The computation results are shown in the following figure

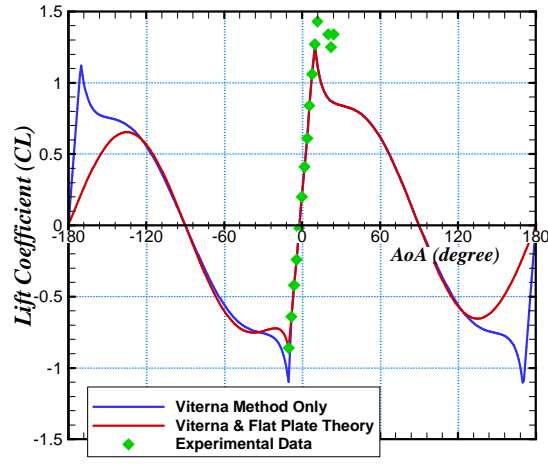


Figure 5: Lift coefficients comparison

It can be observed from the figure that there are discrepancies of results around the peak which are around -170 $^{\circ}$ and 170 $^{\circ}$. Higher peak can be resolved by implementing flat plate theory assumption as shown as red line. As a result, from the figure, it can also be noted the shape is much more sinusoidal when applying the original flat plate theory assumption. The assumption is used in computing lift and drag coefficients from 90 $^{\circ}$ to 180 $^{\circ}$ and in its reflection in negative side of the curve.

The results for drag coefficients are shown in the following figure

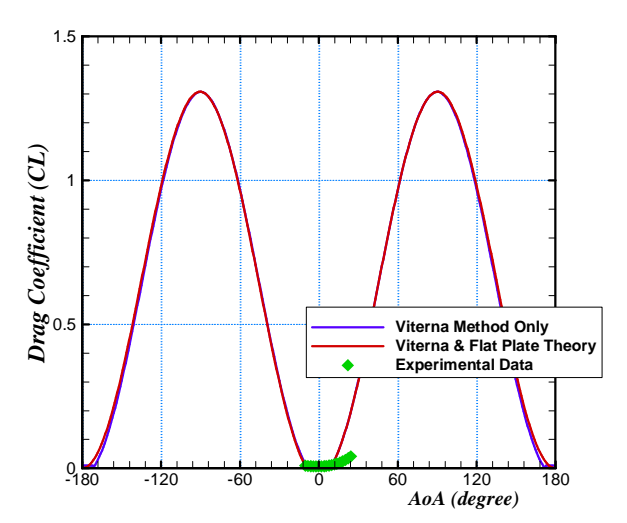


Figure 6: Drag coefficients comparison

From figure above, it can be observed a good agreement between Viterna method and flat plate theory assumption in in terms of shape and magnitude of the curve. The results show that the effect of Viterna method for C_D extrapolation is not significant. Significantly higher C_{Dmax} in the curve can be adjusted using the value of AR as shown in Eq. (7).

5.0 CONCLUSION

In the present study, implementation of lift and drag coefficients experimental data extrapolation using Viterna method and flat plate and theory assumption are performed. It is found that discrepancies can be noticed for lift coefficients while a good agreement can be found in terms of shape and magnitude for drag coefficient. The computation results shown in the present study will be important for determining the Viterna method implementation procedure when using blade element momentum (BEM) method.

ACKNOWLEDGEMENTS

This work was supported by Unggulan Perguruan Tinggi (UPT) research grant from Indonesian Directorate General of Higher Education and Hasanuddin University, Makassar for fiscal year 2016.

REFERENCE

- Abbott, I. H., and Doenhoff, A. E. V. (1949). Theory of Wing Sections Including a Summary of Airfoil Data. New York: Dover Publication, Inc.
- Bianchini, A., Balduzzi, F., Rainbird, J. M., Peiro, J., Graham, J. M. R., Ferrara, G., and Ferrari, L. (2016). An Experimental and Numerical Assessment of Airfoil Polars for Use in Darrieus Wind Turbines Part II: Post-stall Data Extrapolation Methods. *Journal of Engineering for Gas Turbines and Power*, Vol. 138(3), pp: 1–10.

- http://doi.org/10.1115/1.4031270
- 3. Ceyhan, O. (2008). Aerodynamic Design and Optimization of Horizontal Axis Wind Turbines by Using BEM Theory and Genetic Algorithm. Middle East Technical University.
- Døssing, M., Madsen, H. A., and Bak, C. (2011). Aerodynamic Optimization of Wind Turbine Rotors using a Blade Element Momentum Method with Corrections for Wake Rotation and Expansion. Wind Energy, Vol. 15(4), pp: 563–574. http://doi.org/10.1002/we
- Duquette, M. M. (2007). The Development and Application of SimpleFlight, a Variable-Fidelity Flight Dynamics Model. In AIAA Modeling and Simulation Technologies Conference and Exhibit.
- Godreau, C., Caldeira, J., and Campos, J. A. C. F. De. (n.d.). Application of Blade Element Momentum Theory to the Analysis of a Horizontal Axis Wind Turbine. In V Conferência Nacional de Mecânica dos Fluidos, Termodinâmica e Energia (MEFTE). Porto, Portugal.
- Hoburg, W., and Tedrake, R. (2009). System Identification of Post Stall Aerodynamics for UAV Perching. In AIAA Infotech@Aerospace Conference. Seattle, Washington.
- 8. Liu, S., and Janajreh, I. (2012). Development and Application of an Improved Blade Element Momentum Method Model on Horizontal Axis Wind Turbines. *International Journal of Energy and Environmental Engineering*, Vol. 3(30), pp: 1–10
- Matthew, A. B. (2009). A Computational Method for Determining Distributed Aerodynamic Loads on Planforms of Arbitrary Shape in Compressible Subsonic Flow. University of Kansas.
- 10. McCosker, J. (2012). *Design and Optimization of a Small Wind Turbine*. Rensselaer Polytechnic Institute.
- Tangler, J., and Kocurek, J. D. (2005). Wind Turbine Post-Stall Airfoil Performance Characteristics Guidelines for Blade-Element Momentum Methods. In 43rd AIAA Aerospace Sciences Meeting and Exhibit.
- Tangler, J. L. (2004). Insight into Wind Turbine Stall and Post-stall Aerodynamics. Wind Energy, Vol. 7, pp. 247–260. http://doi.org/10.1002/we.122
- 13. Timmer, W. A. (2010). Aerodynamic Characteristics of Wind Turbine Blade Airfoils at High Angles-of-Attack. In *TORQUE 2010: The Science of Making Torque from Wind*. Crete, Greece.
- 14. Tobergte, D. R., and Curtis, S. (2013). Fundamental of Aerodynamics. *Journal of Chemical Information and Modeling*, Vol. 53(9), pp: 1689–1699. http://doi.org/10.1017/CBO9781107415324.004
- Viterna, L. A., and Janetzke, D. C. (1982). Theoretical and Experimental Power From Large Horizontal Axis Wind Turbines (Vol. 82944). Cleveland, Ohio.
- Viterna, L., and Corrigan, R. (1982). Fixed Pitch Rotor Performance of Large Horizontal Axis Wind Turbines. In DOE/NASA Workshop on Large Horizontal Axis Wind Turbines, Cleveland.